https://doi.org/10.3311/PPci.43236 | 1
Creative Commons Attribution

Periodica Polytechnica Civil Engineering

Effect of Metakaolin and Crumb Rubber on the Properties of Roller-Compacted Concrete Containing PP Fibers

Mehran Maghsudi[1], Hamid Beiraghi[1*]

[1] Department of Civil Engineering, MaSh.C., Islamic Azad University, Mahdishahr, Iran
[*] Corresponding author, e-mail: hamid.beiraghi@iau.ac.ir

Received: 31 December 2025, Accepted: 25 July 2026, Published online: 27 August 2026

Abstract

This study investigates the combined effects of metakaolin (MK), crumb rubber (CR), and polypropylene (PP) fibers on the mechanical and durability-related properties of hardened Roller-compacted concrete (RCC). MK was used as a partial cement replacement at levels ranging from 0% to 20% by weight of cement, while PP fibers were incorporated at volume fractions of 0% to 0.2%, and CR was introduced at replacement ratios up to 1% by weight of aggregate. The performance of the mixtures was evaluated through compressive strength, splitting tensile strength, flexural strength, and water absorption tests. The results indicate that the incorporation of MK significantly enhances mechanical performance up to an optimal replacement level of 15%, beyond which strength gains diminish. PP fiber reinforcement notably improves tensile and flexural behavior, with the optimal fiber content identified as 0.1% by volume. Higher fiber dosages resulted in reduced compressive strength due to fiber agglomeration effects. The synergistic use of MK and PP fibers partially mitigates the adverse effects of CR, resulting in improved mechanical performance and acceptable durability characteristics for RCC applications.

Keywords

metakaolin, crumb rubber, mechanical properties, RCC, PP fibers

1 Introduction

Roller-Compacted Concrete (RCC) is a zero-slump cementitious composite consolidated through high-energy vibratory rolling rather than conventional vibration. This placement technique enables rapid construction, high density, and economic efficiency, which has led to its widespread application in pavements, industrial yards, and hydraulic infrastructures [1–3]. Unlike conventional concrete, the performance of RCC is highly sensitive to mixture proportioning, compaction efficiency, and interlayer bonding, making tensile resistance, crack control, and durability critical design considerations [3, 4]. Although RCC exhibits high compressive capacity, its relatively brittle behavior and susceptibility to cracking under repeated or thermal loading remain important limitations in pavement applications.

Enhancement of RCC performance has traditionally relied on optimizing cement content and incorporating supplementary cementitious materials (SCMs) such as fly ash and silica fume [5–7]. These materials improve durability through secondary hydration and pore refinement, leading to reduced permeability and enhanced resistance to sulfate and freeze-thaw attack. However, most studies primarily address compressive strength and durability indices, while improvements in tensile performance and ductility – parameters crucial for fatigue-prone pavements – have received comparatively less integrated attention.

Fiber reinforcement has therefore been introduced to improve crack bridging and post-cracking toughness in RCC systems. Steel, polypropylene (PP), and basalt fibers have demonstrated improvements in flexural strength and fatigue life [8–10]. Among these, PP fibers are particularly attractive due to their chemical stability, low cost, and effectiveness in controlling plastic shrinkage cracking [11–14]. Nevertheless, in low-workability matrices such as RCC, excessive fiber content may cause agglomeration, reduce compaction efficiency, and adversely affect compressive strength. This highlights the need for balanced mixture design strategies that enhance tensile behavior without compromising structural integrity. Parallel to fiber reinforcement, the integration of highly reactive SCMs has been explored to refine the microstructure of cement-based

Cite this article as: Maghsudi, M., Beiraghi, H. "Effect of Metakaolin and Crumb Rubber on the Properties of Roller-Compacted Concrete Containing PP Fibers", Periodica Polytechnica Civil Engineering, 2026. https://doi.org/10.3311/PPci.43236

materials. Metakaolin (MK), a calcined aluminosilicate, exhibits strong pozzolanic reactivity, rapidly consuming calcium hydroxide and forming additional C–S–H and alumina-bearing hydrates [15–18]. Partial cement replacement with MK (typically 5–15%) has been shown to enhance compressive strength, reduce permeability, and densify the ITZ [17, 18]. In RCC, limited studies indicate that MK can improve mechanical performance and durability, particularly when used in conjunction with steel fibers [19, 20].

From a sustainability perspective, the incorporation of recycled materials such as crumb rubber (CR) derived from waste tires has gained increasing attention [21–24]. Rubberized concrete generally exhibits reduced compressive strength due to weak rubber-cement bonding and increased entrapped air; however, it provides enhanced ductility, impact resistance, and energy absorption capacity [22, 25–27]. The magnitude of strength reduction depends on rubber content, particle characteristics, and surface treatment [25, 26]. Recent investigations in conventional concrete suggest that coupling CR with reactive SCMs such as MK may partially compensate for strength losses through matrix densification and improved ITZ quality [27–29]. Despite these promising findings, systematic studies on CR incorporation in RCC remain scarce. More importantly, the interactive effects among CR, MK, and fiber reinforcement in the unique compaction-controlled environment of RCC have not been comprehensively examined.

A critical synthesis of the literature reveals that current knowledge is fragmented: (i) MK has been studied mainly as a strength-enhancing SCM; (ii) PP fibers have been investigated primarily for crack control and toughness; and (iii) CR has been examined as a sustainability-driven aggregate substitute with recognized mechanical penalties. However, there is insufficient understanding of whether microstructural refinement induced by MK and crack-bridging mechanisms provided by PP fibers can synergistically mitigate the adverse mechanical effects of CR in RCC systems. Furthermore, interaction effects under zero-slump compaction conditions remain largely unexplored, representing a significant gap in the design of sustainable, high-performance RCC mixtures.

Accordingly, the present study aims to systematically evaluate the combined influence of MK, CR, and PP fibers on the mechanical and durability-related properties of hardened RCC. The research is structured around the following hypotheses: (i) MK incorporation will enhance compressive strength and reduce water absorption through pozzolanic densification; (ii) PP fibers will improve splitting tensile and flexural performance via crack-bridging mechanisms; and (iii) the simultaneous use of MK and PP fibers will partially offset the strength reduction induced by CR, resulting in a balanced and structurally viable sustainable RCC mixture. By clarifying the interaction mechanisms among these components, this study seeks to advance mixture design strategies for next-generation resilient and environmentally responsible RCC pavements.

2 Material

2.1 Metakaolin

MK is a highly reactive aluminosilicate obtained through the controlled calcination of kaolinite clay. During calcination, the crystalline structure of kaolinite is transformed into an amorphous phase, significantly enhancing its pozzolanic reactivity. This amorphous structure enables effective participation in secondary hydration reactions, leading to improved matrix densification and long-term mechanical performance [30]. The MK employed in this study (Fig. 1) complies with the chemical requirements of ASTM C618. Its oxide composition is presented in Table 1 [31].

Fig. 1 Metakaolan used in the test

Table 1 Chemical composition of MK (% by weight)

No.	Material	%
1	SiO_2	63.51
2	Al_2O_3	21.78
3	CaO	1.66
4	MgO	1.67
5	Na_2O	0.97
6	TiO_2	0.35
7	Fe_2O_3	2.57
8	K_2O	4.69
	SO_3	1.35
9	Loss of ignition	1.2

2.2 Polypropylene fibers

PP fibers are widely used to improve crack control, post-cracking ductility, and impact resistance in cementitious composites. Their low density and hydrophobic nature allow uniform dispersion without increasing mixture weight or promoting segregation. In RCC, fibers contribute primarily to tensile resistance and energy absorption capacity. In the present investigation, 12-mm monofilament PP fibers were incorporated. The principal physical and mechanical properties of the fibers are summarized in Table 2.

2.3 Aggregates

Aggregates constitute approximately 60–75% of the total volume of RCC and strongly influence both fresh compactability and hardened performance. A well-graded aggregate skeleton is essential to minimize void content and ensure effective compaction under vibratory loading [32]. The nominal maximum aggregate size (NMAS) adopted in this study was within the commonly recommended range for RCC pavements (12.5–19 mm) [33]. The gradation curve was designed in accordance with ACI 325.10R-95 recommendations [34], ensuring a balanced distribution of coarse and fine particles to optimize packing density and reduce paste demand. The adopted gradation is illustrated in Fig. 2.

Table 2 Characteristics PP fibers

Quantity	Characteristic
0.95	Density (g/m^3)
38	Diameter (mm)
3.5	Tensil strain to fracture (%)
12	Length (mm)
165	Degree of fusion (°C)
0	Water absorption (%)
400	Strength (MPa)

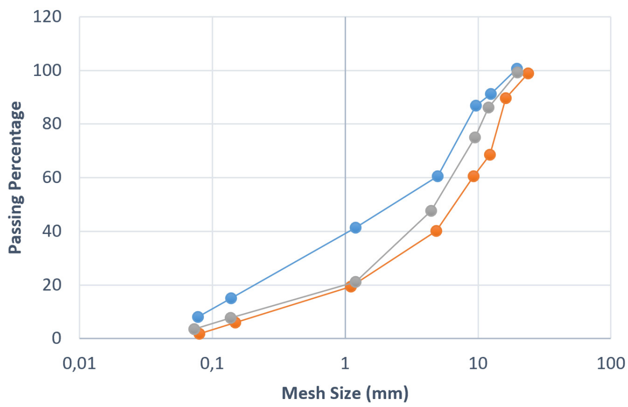

Fig. 2 The gradation pattern used in this study

2.4 Crumb rubber

CR was obtained from recycled automobile tires and sieved to achieve particle sizes between 4.75 and 15 mm. The specific gravity ranged from 1.06 to 1.13. In this study, CR was incorporated as a mass-based partial replacement of coarse aggregate at levels of 5% and 10% by weight of coarse aggregate, corresponding to 25 kg/m^3 and 50 kg/m^3, respectively. The replacement basis was deliberately selected as mass-based to ensure precise batching control, reproducibility, and consistency with common RCC production practices. This approach eliminates ambiguity associated with volumetric conversions arising from the significant density difference between natural aggregates and rubber particles.

2.5 Water-reducing admixture

A third-generation naphthalene-based water-reducing admixture was used at a fixed dosage of 1% by mass of cementitious materials [35]. The admixture was added at the final stage of mixing to ensure uniform dispersion and optimal workability prior to compaction.

3 Tested matrix

MK was incorporated as a partial replacement of cement at levels of 0%, 5%, 15%, and 20% by weight of cement. PP fibers were introduced at volumetric contents of 0%, 0.1%, and 0.2% of the total mixture volume. CR was used as a 5% and 10% mass-based replacement of coarse aggregate (25 and 50 kg/m^3, respectively). By combining four MK levels, three fiber contents, and three rubber replacement levels (including control without rubber), a total of 36 distinct mix designs were produced and evaluated (Table 3). The relatively large number of mixtures was intentionally selected to enable systematic evaluation of individual effects as well as interaction effects among MK, PP fibers, and CR in RCC. This factorial design allows comprehensive assessment of synergistic or antagonistic mechanisms influencing mechanical and durability-related performance. Micro-silica was incorporated in sludge form after initial blending of dry materials and water. Fibers were gradually introduced to ensure proper dispersion, followed by aggregates. Cement was then added under continuous mixing, and finally the superplasticizer was introduced immediately prior to casting. Mixing continued for two additional minutes to ensure homogeneity before specimen preparation.

Table 3 Mix ratio specification (kg/m^3)

Mix No.	Water	Cement	Sand	Aggregate	PP Fibers	CR	MK	Water-reducing admixture
1	140	350	700	1200	0	0	0	1
2	140	350	700	1200	0.5	0	0	1
3	140	350	700	1200	1	0	0	1
4	140	350	700	1180	0	25	0	1
5	140	350	700	1180	0.5	25	0	1
6	140	350	700	1180	1	25	0	1
7	140	350	700	1160	0	40	0	1
8	140	350	700	1160	0.5	40	0	1
9	140	350	700	1160	1	40	0	1
10	140	332.5	700	1200	0	0	17.5	1
11	140	332.5	700	1200	0.5	0	17.5	1
12	140	332.5	700	1200	1	0	17.5	1
13	140	332.5	700	1180	0	25	17.5	1
14	140	332.5	700	1180	0.5	25	17.5	1
15	140	332.5	700	1180	1	25	17.5	1
16	140	332.5	700	1160	0	40	17.5	1
17	140	332.5	700	1160	0.5	40	17.5	1
18	140	332.5	700	1160	1	40	17.5	1
19	140	315	700	1200	0	0	35	1
20	140	315	700	1200	0.5	0	35	1
21	140	315	700	1200	1	0	35	1
22	140	315	700	1180	0	25	35	1
23	140	315	700	1180	0.5	25	35	1
24	140	315	700	1180	1	25	35	1
25	140	315	700	1160	0	40	35	1
26	140	315	700	1160	0.5	40	35	1
27	140	315	700	1160	1	40	35	1
28	140	297.5	700	1200	0	0	52.5	1
29	140	297.5	700	1200	0.5	0	52.5	1
30	140	297.5	700	1200	1	0	52.5	1
31	140	297.5	700	1180	0	25	52.5	1
32	140	297.5	700	1180	0.5	25	52.5	1
33	140	297.5	700	1180	1	25	52.5	1
34	140	297.5	700	1160	0	40	52.5	1
35	140	297.5	700	1160	0.5	40	52.5	1
36	140	297.5	700	1160	1	40	52.5	1

4 Fresh concrete tests

The freshly prepared concrete mixtures were evaluated in accordance with ASTM C1437-15, Standard Test Method for Flow of Hydraulic Cement Mortar. This procedure determines the flowability (workability) of the mixture, which serves as a key indicator of its ease of placement and compaction. Although RCC generally exhibits substantially lower workability than conventional vibrated concrete, maintaining adequate consistency remains essential for achieving proper compaction and structural integrity [36]. Even in low-slump RCC systems, this test provides meaningful insight into the mixture's response to external energy input during compaction and its overall handling characteristics (Fig. 3).

5 Comparison of compressive strength test results

The preparation of prismatic, cubic, and cylindrical specimens was carried out in accordance with

Fig. 3 slump test for fresh concrete

ASTM C31/C31M-12 [37] and ASTM C511-13 [38]. Immediately after casting, the specimens were covered with two layers of plastic sheeting to prevent moisture loss and were stored for 24 hours in a temperature-controlled environment maintained at 22 ± 2 °C. Following this initial curing period, the specimens were demolded and transferred to a saturated limewater bath to ensure proper hydration and to minimize potential leaching of $Ca(OH)_2$ from the cementitious matrix (Fig. 4). Compressive strength testing was performed using a 2,000 kN universal testing machine under displacement-controlled loading conditions. A uniaxial loading rate of 0.3 MPa/s was applied and regulated through the machine's crosshead movement. For each mixture, the reported compressive strength corresponds to the average value obtained from three replicate cubic specimens. The final compressive strength for each mix design was subsequently calculated based on the experimental measurements using Eq. (1).

$$S = P / A , \quad (1)$$

where A is the compression loaded area's cross-section and P is the load.

Fig. 4 Specimen preparation

5.1 Compressive strength without PP fibers

A comparative evaluation of compressive strength at 7, 28, and 90 days – considering various MK replacement levels combined with different CR contents and in the absence of PP fibers – revealed that the incorporation of 15% MK resulted in the most favorable mechanical performance (Fig. 5). The mixture containing 15% MK without CR achieved the highest 28-day compressive strength of 35 MPa, indicating that this replacement level provided an optimal balance between filler effects and pozzolanic reactivity. At this dosage, MK contributed to matrix densification through secondary C–S–H formation and refinement of the ITZ, thereby enhancing load transfer efficiency within the compacted RCC matrix. However, the incorporation of CR led to a systematic reduction in compressive strength. For each 5% increase in CR content (by mass of coarse aggregate), the compressive strength decreased by approximately 10%. This reduction can be attributed to the significantly lower stiffness and strength

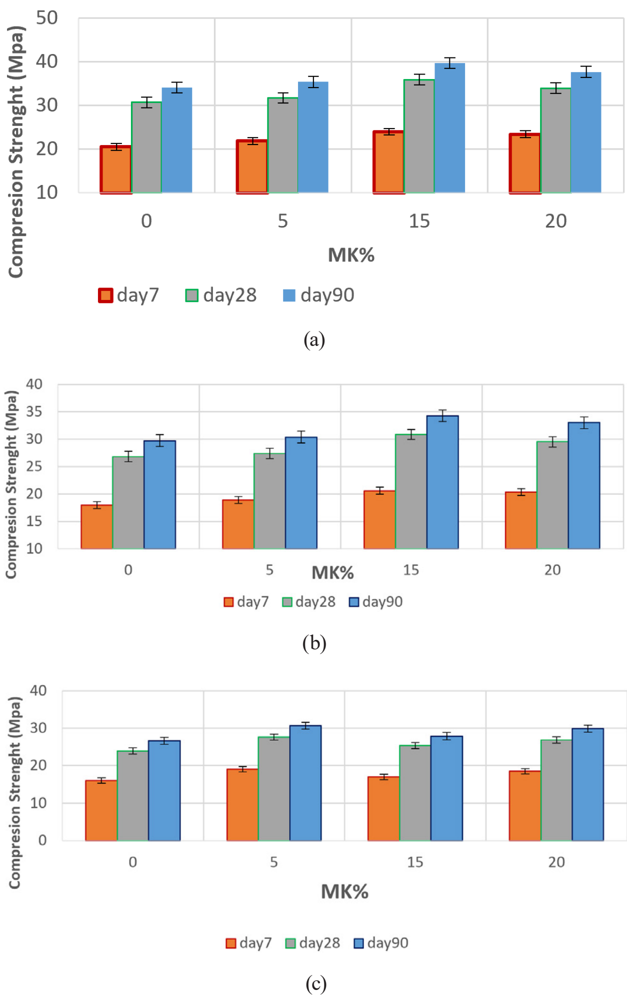

Fig. 5 Compressive strength of mixtures without PP fibers:
(a) 0% crumb rubber, (b) 5% crumb rubber, (c) 10% crumb rubber

of rubber particles compared to natural aggregates, which alters the internal stress distribution under compressive loading. Moreover, the hydrophobic nature and smooth surface texture of CR weaken the aggregate-paste interfacial bonding, resulting in a more compliant ITZ and promoting microcrack initiation under load. In the relatively low-paste RCC system, where mechanical interlock and aggregate skeleton stability play a dominant role, partial replacement of stiff mineral aggregate with deformable rubber particles directly reduces the effective load-bearing capacity of the composite.

Despite this strength reduction, the coefficient of variation (COV) of compressive strength remained below 7% for all mixtures, demonstrating good repeatability and experimental consistency across the tested matrix. The limited statistical dispersion confirms that the observed performance trends are structurally driven and reproducible rather than a consequence of experimental variability.

5.2 Compressive strength with 0.1% PP fibers

A comparative evaluation of the 7-, 28-, and 90-day compressive strength results – considering different MK replacement levels in combination with varying CR dosages and the incorporation of 0.1% PP fibers by volume – demonstrated that the mixture containing 15% MK exhibited the most favorable performance (Fig. 6). The mix incorporating 15% MK without CR achieved a 28-day compressive strength of 38 MPa, representing the highest value within this subgroup. In contrast, the addition of CR resulted in a progressive reduction in compressive strength. Specifically, each 5% increase in CR content (by mass of coarse aggregate) produced an approximate 10% decrease in compressive strength. Despite this reduction, the overall strength development trend remained consistent across curing ages, indicating that the beneficial effect of MK on matrix densification persisted even in the presence of rubber particles.

5.3 Compressive strength with 0.2% PP fibers

As shown in Fig. 7, mixtures incorporating 0.2% PP fibers by volume exhibited lower compressive strength compared with those containing 0.1% fibers. This reduction may be attributed to reduced workability and potential fiber clustering at higher dosages, which can adversely affect matrix homogeneity and compaction efficiency in RCC systems. The results further confirm that the optimal MK replacement level remains 15%. At this dosage, the 28-day compressive strength of the mixture without

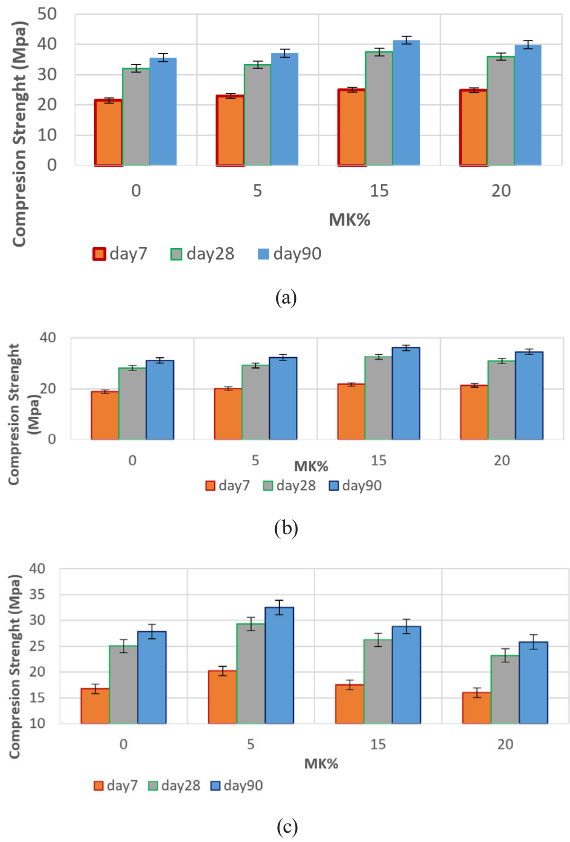

Fig. 6 Compressive strength in mixtures incorporating 0.1% PP fibers: (a) 0% crumb rubber, (b) 5% crumb rubber, (c) 10% crumb rubber

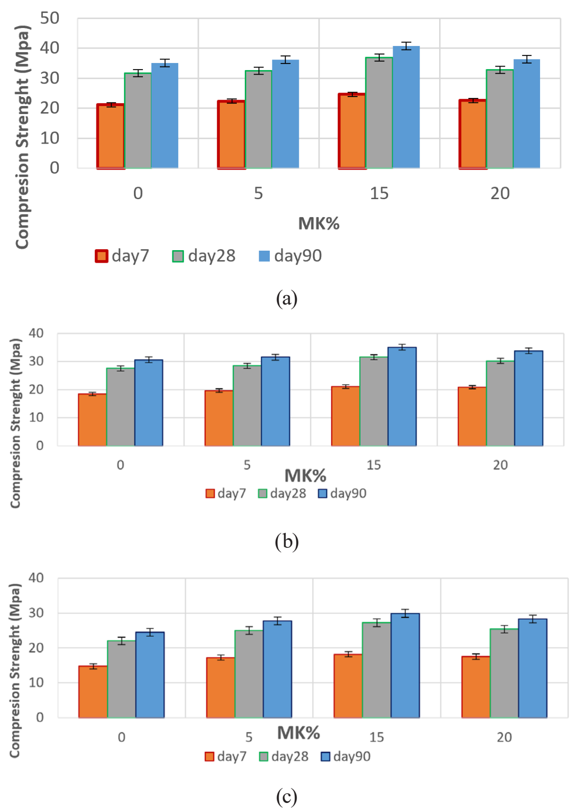

Fig. 7 Compressive strength in mixtures incorporating 0.2% PP fibers: (a) 0% crumb rubber, (b) 5% crumb rubber, (c) 10% crumb rubber

CR reached 36.8 MPa. Although strength values remained comparatively high at this fiber content, the marginal gain in crack-bridging capacity did not compensate for the slight reduction in compressive performance associated with increased fiber volume.

5.4 The effect of different amounts of fibers on compressive strength

Fig. 8 presents a comparison of compressive strength results for mixtures containing 5% CR in combination with varying MK replacement levels and different PP fiber dosages. The results indicate that the highest compressive strength was achieved in the mixture incorporating 15% MK and 0.1% PP fibers, demonstrating a favorable interaction between pozzolanic matrix refinement and controlled fiber reinforcement. The maximum compressive strength within this category reached 32.5 MPa. The superior performance observed for the mixture containing 15% MK and 0.1% PP fibers in the presence of 5% CR can be attributed to a balanced interaction among matrix densification, microcrack control, and limited rubber-induced stiffness reduction. MK enhances compressive performance through accelerated secondary pozzolanic reactions, leading to additional C–S–H formation, refinement of the pore structure, and improved ITZ characteristics. Simultaneously, a 0.1% PP fiber dosage provides effective microcrack arresting and improved stress redistribution without inducing fiber agglomeration or compromising compaction quality-effects that may occur at higher fiber contents. Although CR incorporation reduces stiffness due to its lower elastic modulus relative to mineral aggregates, the optimized MK–fiber combination partially compensates for this reduction by improving stress transfer within the composite matrix. Fig. 9 further illustrates the combined influence of varying CR and MK contents on compressive strength at 28 days for mixtures incorporating 0.1% PP fibers.

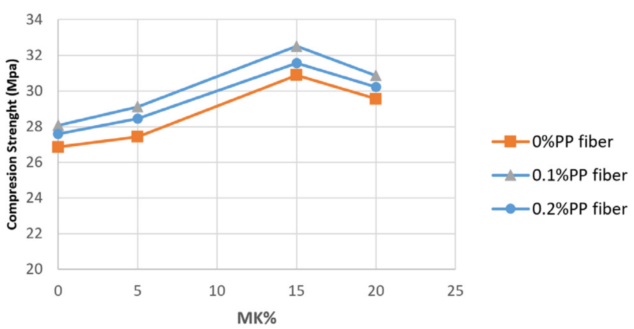

Fig. 8 Effect of MK and PP fibers on compressive strength for mixtures containing 5% CR at 28 days

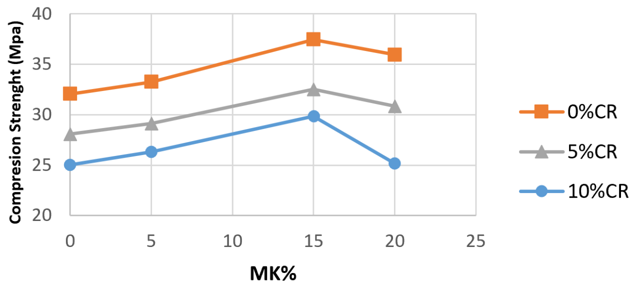

Fig. 9 Influence of CR and MK contents on 28-day compressive strength in mixtures incorporating 0.1% PP fibers

6. Splitting tensile strength

In this study, cylindrical specimens were cast, cured, and tested in accordance with ASTM C496 [39] to determine the splitting tensile strength (STS) of the concrete mixtures. The STS tests were conducted using a digital compression testing machine with a capacity of 2,000 kN, and the reported values represent the average of three replicate specimens. Splitting tensile strength is conventionally evaluated using cylindrical specimens subjected to a diametral compressive load, which induces indirect tensile stresses along the vertical diameter. This standardized procedure enables a reliable assessment of the tensile resistance of concrete, particularly for mixtures in which brittleness, microcracking behavior, or modifications to the cementitious matrix are of primary interest.

$$Fct = \frac{2p}{\pi DL} \tag{2}$$

The tensile strength of concrete is denoted as Fct where D, L, and p represent the specimen diameter, specimen length, and maximum applied load, respectively. Splitting tensile strength tests were performed on cylindrical specimens with dimensions of 150 mm in diameter and 300 mm in height at curing ages of 7, 28, and 90 days, following the Brazilian splitting test procedure. Prior to testing, the specimens were removed from the curing tank, surface-dried, and positioned under diametral loading using a hydraulic loading system to induce tensile failure along the vertical axis. The corresponding tensile strength values were calculated using the standard analytical expression given in Eq. (2). Fig. 10 presents the results of the splitting tensile strength tests for mixtures incorporating MK and CR without fiber reinforcement. The results indicate that the mixture containing 15% MK and 5% CR achieved the highest splitting tensile strength. Similar trends are observed in Figs. 11 and 12 for mixtures incorporating 0.1% and 0.2% PP fibers, respectively. A comparative evaluation of mixtures with

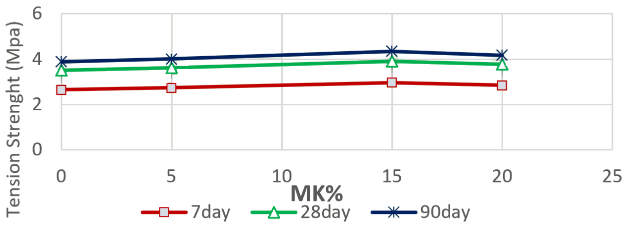

(a)

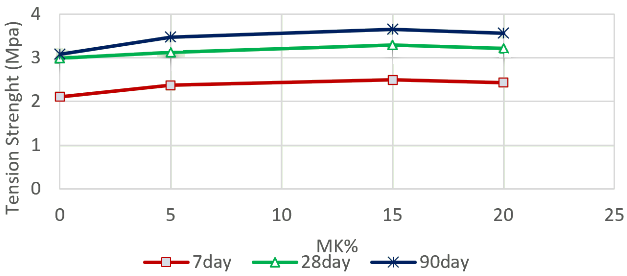

(b)

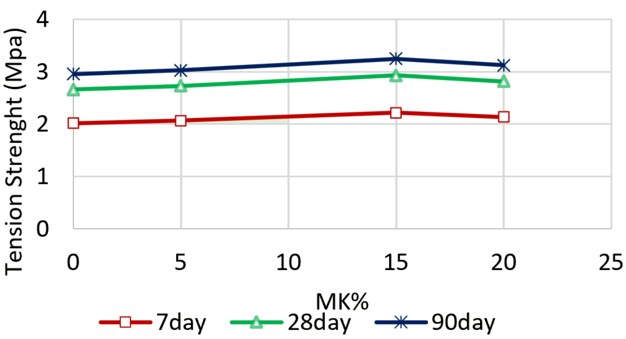

(c)

Fig. 10 Results of split tensile test with varying amounts of MK and CR and no fiber: (a) 0% crumb rubber, (b) 5% crumb rubber, (c) 10% crumb rubber

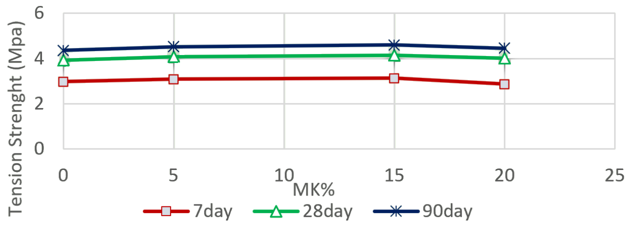

(a)

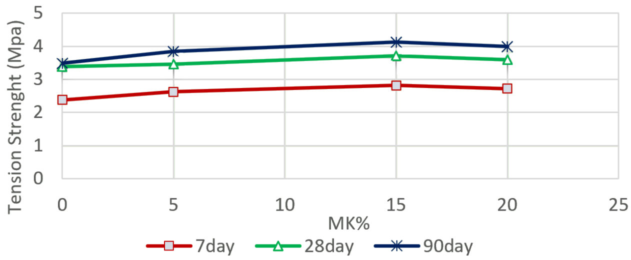

(b)

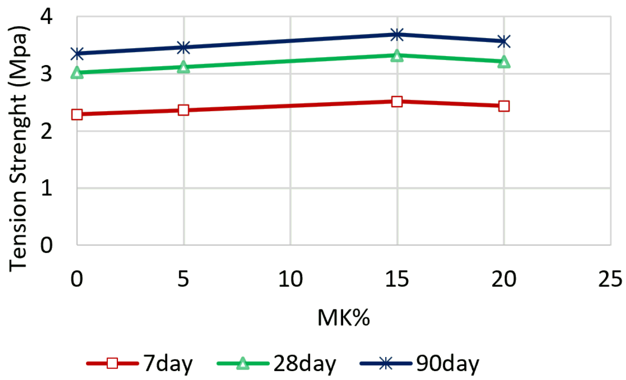

(c)

Fig. 11 Results of split tensile test with varying amounts of MK and CR and 0.1% fiber: (a) 0% crumb rubber, (b) 5% crumb rubber, (c) 10% crumb rubber

varying MK replacement levels and PP fiber dosages – while maintaining a constant CR content of 5% – indicates that the optimum fiber content is 0.1% PP, yielding a maximum splitting tensile strength of 3.7 MPa. The enhancement in splitting tensile strength observed for the mixture containing 15% MK and 5% CR can be attributed to the synergistic effects of matrix densification and controlled deformability. MK promotes secondary pozzolanic reactions, leading to the formation of additional C–S–H gel and refinement of the ITZ, thereby improving stress transfer within the cementitious matrix. Simultaneously, CR enhances energy absorption capacity and contributes to crack-bridging under tensile loading, reducing the tendency toward brittle fracture. The superior performance obtained with 0.1% PP fiber is associated with its adequate dispersion and effective micro-crack-arresting capability without inducing fiber agglomeration or matrix discontinuities, phenomena that may occur at higher fiber dosages. The combined action of these mechanisms results in a balanced composite system with enhanced tensile resistance. Fig. 13 presents a comparative analysis of the splitting tensile strength of mixtures containing varying MK replacement levels and PP fiber contents in combination with 10% CR.

7 Flexural strength test

For each mixture, prismatic beam specimens were cast and tested in accordance with ASTM C293 [40] to determine flexural strength using the center-point loading method. All specimens were subjected to monotonic, displacement-controlled loading, and the reported flexural strength values represent the average of three identical beams. During testing, a concentrated vertical load was applied at the midspan of each simply supported specimen, and the corresponding ultimate load at failure was recorded. The flexural tensile strength was calculated using the following relationship:

$$fz = Fl / bh2 , \tag{3}$$

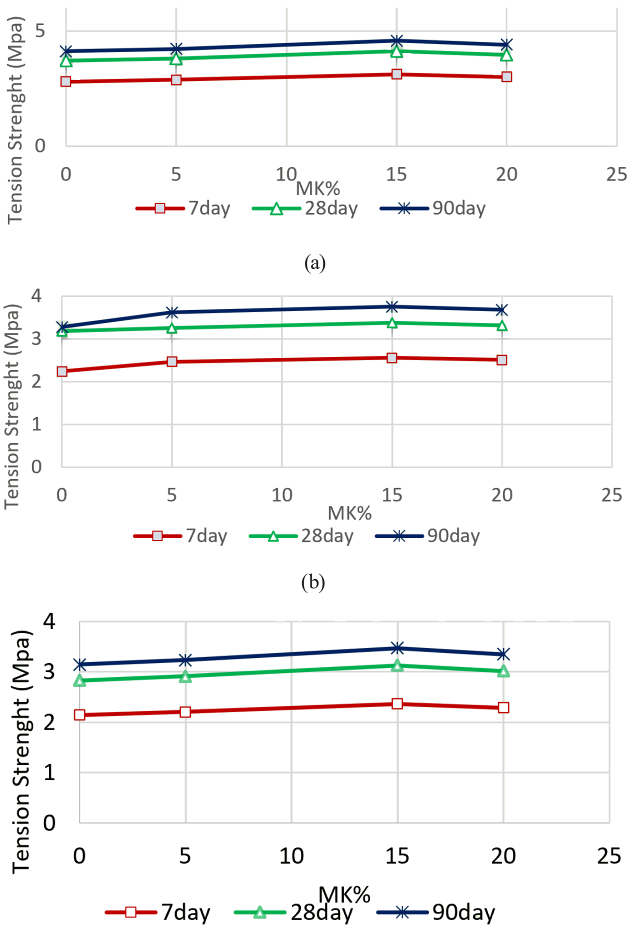

Fig. 12 Results of split tensile test with varying amounts of MK and CR and 0.2% fiber: (a) 0% crumb rubber, (b) 5% crumb rubber, (c) 10% crumb rubber

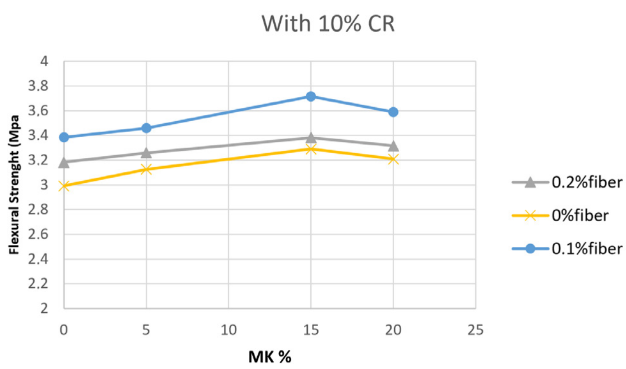

Fig. 13 Comparison of split tensile test with varying amounts of MK and PP fiber with 10% CR

where *ft* denotes the flexural tensile strength (modulus of rupture), *F* is the maximum applied load at failure, *l* is the span length between supports, and *b* and *h* represent the width and height of the beam cross section, respectively. Fig. 14 presents the flexural performance of mixtures incorporating varying CR contents in combination

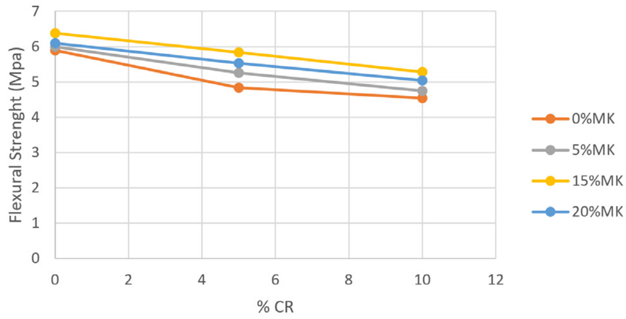

Fig. 14 Flexural test results with different amounts of CR and 0.1% fibers

with 0.1% PP fiber. The results demonstrate that the mixture containing 15% MK consistently achieves the highest flexural strength at curing ages of 7, 28, and 90 days. This trend underscores the significant contribution of MK to matrix densification and enhanced fiber–matrix interfacial bonding, both of which are critical to flexural resistance. In contrast, partial replacement of fine aggregate with approximately 10% CR results in an average reduction of nearly 10% in flexural strength. This decline is primarily attributed to the relatively low stiffness and elastic modulus of rubber particles compared to mineral aggregates. The inclusion of CR introduces localized zones of deformability within the cementitious matrix, which diminishes stress-transfer efficiency under bending and reduces resistance to tensile stresses developed at the extreme fiber of the beam section. The superior flexural behavior observed in mixtures containing 15% MK can be explained by intensified pozzolanic reactions, which promote the formation of additional C–S–H gel, refine pore structure, and densify the ITZ. These microstructural improvements enhance load-transfer mechanisms and improve the bond quality between PP fibers and the surrounding matrix, thereby increasing crack-bridging effectiveness under flexural loading. Conversely, the reduction in flexural strength associated with 10% CR replacement is linked to the hydrophobic surface characteristics and lower rigidity of rubber particles, which may weaken the ITZ and reduce composite stiffness. Although CR can contribute to energy absorption and post-cracking ductility, its presence at higher replacement levels adversely affects the initial flexural capacity due to diminished matrix continuity and reduced tensile stress resistance.

8 The water absorption

The water absorption of hardened concrete was determined in accordance with ASTM C642-06 [41]. After 28 days of water curing, each specimen was removed from the curing tank and weighed in the saturated surface-dry (SSD) condition to obtain its mass. The specimen was then oven-dried at 100–110 °C for 24 hours to remove free moisture. After cooling to room temperature, the oven-dry mass was recorded. Water absorption was calculated based on the difference between the saturated and oven-dry masses using the following expression:

$$\text{Water absorption} = \frac{m - m_0}{m_0} \times 100 , \quad (4)$$

where m is the wet sample weight and m_0 is the dry sample weight.

The results indicate that increasing the MK content leads to a gradual reduction in water absorption up to an optimal replacement level of 15%, beyond which the improvement becomes marginal (Fig. 15). Although the reduction is moderate, it reflects the pore-refining effect of MK through secondary pozzolanic reactions and additional C–S–H formation. The reference mixture without fiber, MK, or CR exhibits a water absorption of approximately 3.2%, whereas mixtures incorporating up to 15% MK show a reduced value of about 2.8%, indicating enhanced matrix densification and reduced capillary porosity. In contrast, the incorporation of PP fibers results in a slight increase in water absorption. This behavior can be attributed to the formation of interfacial voids and localized microchannels around dispersed fibers, particularly if fiber distribution is not perfectly uniform. Similarly, the inclusion of CR leads to a more pronounced increase in water absorption. For example, mixtures containing 10% CR exhibit an absorption value of approximately 4.5%. This increase is associated with the hydrophobic surface characteristics, lower stiffness, and intrinsic porosity of rubber particles, which may weaken the ITZ, disrupt matrix continuity, and increase overall permeability. Overall, the results demonstrate that MK improves durability-related properties by refining pore structure, whereas CR and, to a lesser extent, PP fibers may increase permeability due to interfacial discontinuities and reduced matrix compactness.

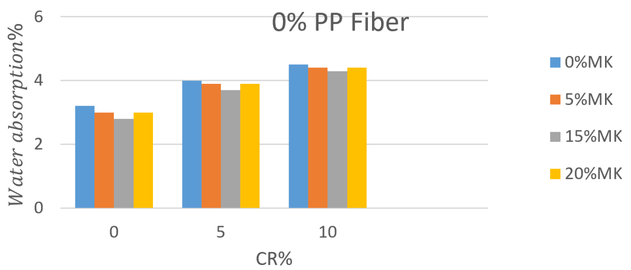

(a)

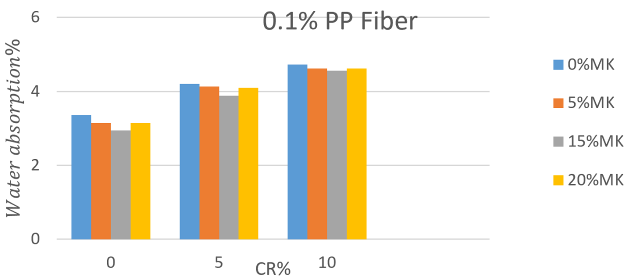

(b)

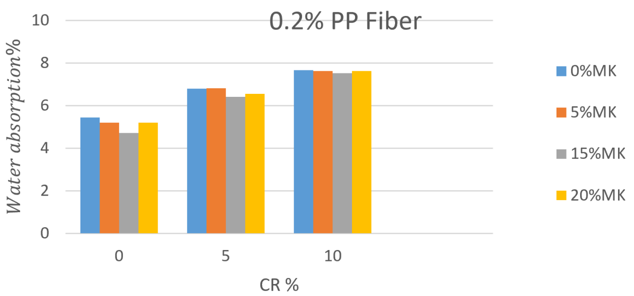

(c)

Fig. 15 Water absorption test results for 28 day samples: (a) 0% PP fiber, (b) 0.1% PP fiber, (c) 0.2% PP fiber

9 Compressive and tensile strength relation

Fig. 16 illustrates the relationship between compressive strength and splitting tensile strength for all tested mixtures. Regression analysis was performed using a nonlinear power-law model, which provided the best statistical fit to the experimental dataset. The resulting predictive expression is given by:

$$f_{sp} = 0.192 f'_c \wedge 0.778 , \quad (5)$$

where f_{sp} is the splitting tensile strength (MPa) and f'_c is the cylindrical compressive strength (MPa). The cylindrical strength was calculated as 0.8 times the measured cube compressive strength to ensure compatibility with standard code-based formulations. The proposed

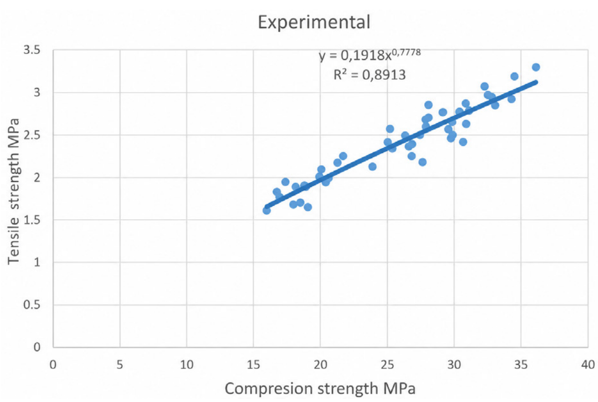

Fig. 16 Regression relationship between compressive strength and splitting tensile strength

regression model demonstrated a coefficient of determination $R^2 = 0.89$, indicating a strong correlation between compressive and tensile strength across the investigated mixtures. In addition, the root mean square error (RMSE) of the model was found to be relatively low compared to the experimental strength range, confirming the predictive stability of the equation. The residual distribution did not exhibit systematic bias with increasing strength level, suggesting that the power-law formulation appropriately captures the nonlinear dependence of tensile strength on compressive strength in RCC incorporating MK, PP fibers, and CR. To further assess the validity of existing predictive approaches, the experimental results were compared with commonly adopted design-code formulations developed for conventional vibrated concrete. The expressions recommended by ACI 318-11 [42], Eurocode 2-04 [43], NZS 3101 [44], JCI-08 [45], and AS 3600-18 [46] are summarized in Table 4. Fig. 17 presents a comparative evaluation between experimentally measured splitting tensile strengths and code-based predictions.

Although the ACI 318 formulation exhibited the closest overall agreement with the experimental results, noticeable deviations were observed for mixtures containing CR. Most code-based expressions either underestimated or overestimated the tensile strength, particularly at higher compressive strength levels. This discrepancy can be attributed to the fact that existing design provisions were

Table 4 Design expressions for estimating the splitting tensile strength of conventional concrete, as recommended by current codes

Code Name	Splitting tensile strength formula (MPa)
ACI 318-11	$0.53\ (f'_c)$^0.5
Eurocode 2-04	$0.3\ (f'_c)$^0.667
NZS 3101	$0.44\ (f'_c)$^0.5
JCI-08	$0.13\ (f'_c)$^0.85
AS 3600-18	$0.36\ (f'_c)$^0.5

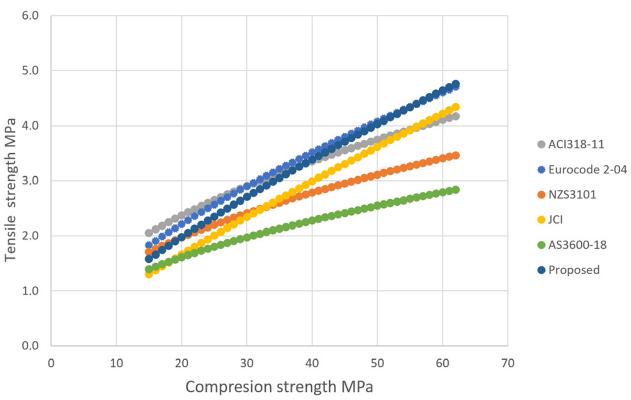

Fig. 17 Comparison between the experimental results and code-based formulations for predicting splitting tensile strength

calibrated using conventional vibrated concrete without rubber inclusions and with different paste volumes and compaction mechanisms.

In RCC systems, mechanical interlock of aggregates and reduced paste content play a dominant structural role, while the presence of CR modifies stiffness compatibility and alters crack initiation behavior within the ITZ. Consequently, the compressive-tensile strength relationship deviates from that assumed in conventional concrete models. The exponent obtained in the present regression (0.778) reflects this modified stress-transfer mechanism and suggests that tensile strength in rubberized RCC exhibits a slightly stronger nonlinear dependence on compressive strength compared to several code-based square-root formulations. Overall, the proposed model provides improved predictive capability for the specific material system investigated in this study and may serve as a more appropriate estimation tool for RCC mixtures incorporating MK and CR within the investigated strength range.

10 Conclusions

Based on the experimental investigation of RCC mixtures incorporating MK, CR, and PP fibers, the following conclusions can be drawn:

The partial replacement of cement with MK significantly enhances the mechanical properties of RCC up to an optimal level of 15%, attributed to improved pozzolanic activity and matrix densification.

PP fibers play a critical role in improving the tensile and flexural performance of RCC, with the optimal fiber content identified as 0.1% by volume. Increasing the fiber content to 0.2% resulted in reduced compressive strength, likely due to fiber clustering and reduced workability.

The incorporation of CR generally leads to a reduction in compressive and flexural strength, primarily due to the lower stiffness and weaker interfacial bonding of rubber particles compared to natural aggregates.

Despite strength reductions, mixtures containing CR exhibited acceptable mechanical performance when combined with MK and PP fibers, demonstrating a beneficial synergistic effect.

Water absorption results showed that MK reduced permeability up to the optimal replacement level, while PP fibers and CR slightly increased absorption due to increased interfacial voids.

The combined use of MK and PP fibers is effective in compensating for the mechanical drawbacks associated with CR incorporation, making this approach suitable for sustainable RCC applications.

References

[1] ACI Committee 207 "ACI 207.5R-99: Roller-Compacted Mass Concrete", American Concrete Institute, 2005.

[2] Tufail, R. F., Feng, X., Farooq, D., Abdelmelek, N., Lublóy, É. "Behavior and Strength Predictions for CFRP Confined Rubberized Concrete under Axial Compression", Periodica Polytechnica Civil Engineering, 66(1), pp. 164–178, 2022. https://doi.org/10.3311/PPci.1465

[3] Medine, M., Trouzine, H., De Aguiar, J. B. "Fresh State Properties of Concrete Incorporating Scrap Tire Rubber", Periodica Polytechnica Civil Engineering, 60(4), pp. 610–617, 2016. https://doi.org/10.3311/PPci.8727

[4] Aghaeipour, A., Madhkhan, M. "Mechanical Properties and Durability of Roller Compacted Concrete Pavement (RCCP): A Review", Road Materials and Pavement Design, 21(7), pp. 1775–1798, 2020. https://doi.org/10.1080/14680629.2019.1579754

[5] Amin, M. N., Mohammed, B. S. "Recent Advances in Roller Compacted Concrete: Sustainability and Performance Perspectives", Journal of Cleaner Production, 345, 130978, 2023.

[6] Lopez-Uceda, A., Agrela, F., Cabrera, M., Ayuso, J., López, M. "Mechanical Performance of Roller Compacted Concrete with Recycled Concrete Aggregates", Road Materials and Pavement Design, 19(1), pp. 36–55, 2018. https://doi.org/10.1080/14680629.2016.1232659

[7] Calis, G., Yıldızel, S. A. "Investigation of Roller Compacted Concrete: Literature Review", Challenge Journal of Concrete Research Letters, 10(3), pp. 63–74, 2019. https://doi.org/10.20528/cjcrl.2019.03.003

[8] Selvam, M., Debbarma, S., Singh, S., Shi, X. "Utilization of Alternative Aggregates for Roller Compacted Concrete Pavement: a state-of-the-art review", Construction and Building Materials, 317, 125838, 2021. https://doi.org/10.1016/j.conbuildmat.2021.125838

[9] Sun, H., Qian, J., Yang, Y., Fan, C., Yue, Y. "Optimization of gypsum and slag contents in blended cement containing slag", Cement and Concrete Composites, 112, 103674, 2020. https://doi.org/10.1016/j.cemconcomp.2020.103674

[10] Tang, W., Wang, R., Zhang, H. "Enhancing Mechanical Properties of Fiber-Reinforced Roller Compacted Concrete", Materials Today Communications, 31, 103544, 2022.

[11] Kalbande, M. N., Panse, T. G., Gaidhani, Y. A., Balpande, R. S., Patil, T. R., Kakade, N. T., Nair, S., Shelke, N., Isleem, H. F., Vairagade, V. S. "Hybrid Machine Learning Based Strength and Durability Predictions of Polypropylene Fiber-Reinforced Graphene Oxide Based High-Performance Concrete", Iran Journal of Science and Technology, Transactions of Civil Engineering, 50(1), pp. 509–529, 2026. https://doi.org/10.1007/s40996-025-01852-z

[12] Tahir, M., Hameed, R., Riaz, M. R., Waqas, M. "Bond Stress-Slip Behavior of Hybrid Fiber-Reinforced Recycled Aggregate Concrete Using Beam Test", Iran Journal of Science and Technology, Transactions of Civil Engineering, 47(2), pp. 753–760, 2023. https://doi.org/10.1007/s40996-023-01042-9

[13] Resan, S. F., Chassib, S. M., Zemam, S. K., Madhi, M. J. “New Approach of Concrete Tensile Strength Test", Case Studies in Construction Materials, 12, e00347, 2020. https://doi.org/10.1016/j.cscm.2020.e00347

[14] Ma, K., Liu, J., Jiang, C., Ma, X.-F., Huang, L.-H., He, C.-Z., Qi, C.-Q. "Compressive and Tensile Strength of Polymer-Based Fiber Composite Sand", Journal of Central South University, 29(2), pp. 528–545, 2022. https://doi.org/10.1007/s11771-022-4909-9

[15] Mindess, S., Young, F. J., Darwin, D. "Concrete", Prentice Hall, 2003.

[16] Al-Hashem, M. N., Amin, M. N., Ajwad, A., Afzal, M., Khan, K., Faraz, M. I., Qadir, M. G., Khan, H. "Mechanical and Durability Evaluation of Metakaolin as Cement Replacement Material in Concrete", Materials, 15(22), 7868, 2022. https://doi.org/10.3390/ma15227868

[17] Dinakar, P., Sahoo, P. K., Sriram, G. "Effect of Metakaolin Content on the Properties of High Strength Concrete", International Journal of Concrete Structures and Materials, 7(3), pp. 215–223, 2013. https://doi.org/10.1007/s40069-013-0045-0

[18] Ferreira, R. M., Castro-Gomes, J. P., Costa, P., Malheiro, R. "Effect of Metakaolin on the Chloride Ingress Properties of Concrete", KSCE Journal of Civil Engineering, 20(4), pp. 1375–1384, 2016. https://doi.org/10.1007/s12205-015-0131-8

[19] Ünverdi, M., Kaya, Y., Mardani, N., Mardani, A. "Investigation of the Microstructural and Mechanical Properties of Fiber-Reinforced Roller-Compacted Concrete under High-Temperature Exposure", Materials, 18(11), 2430, 2025. https://doi.org/10.3390/ma18112430

[20] Güneyisi, E., Gesoğlu, M., Mermerdaş, K. "Improving Strength, Drying Shrinkage, and Pore Structure of Concrete Using Metakaolin", Materials and Structures, 41(5), pp. 937–949, 2007. https://doi.org/10.1617/s11527-007-9296-z

[21] Khern, Y. C., Paul, S. C., Kong, S. Y., Babafemi, A. J., Anggraini, V., Miah, M. J., Šavija, B. "Impact of Chemically Treated Waste Rubber Tire Aggregates on Mechanical, Durability and Thermal Properties of Concrete", Frontiers in Materials, 7, 90, 2020. https://doi.org/10.3389/fmats.2020.00090

[22] Eissa, M., Habib, A., Al Houri, A., Alibrahim, B. "Recent Efforts on Investigating the Effects of Recycled Rubber Content on the Mechanical Properties of Structural Concrete", Discover Civil Engineering, 1(1), 16, 2024. https://doi.org/10.1007/s44290-024-00017-7

[23] Feng, L.-Y., Chen, A.-J., Liu, H.-D. "Effect of Waste Tire Rubber Particles on Concrete Abrasion Resistance Under High-Speed Water Flow", International Journal of Concrete Structures and Materials, 15(1), 37, 2021. https://doi.org/10.1186/s40069-021-00475-8

[24] Castillo, R., Alva, A., París-Viviana, O., Bosch, M. "A Systematic Bibliometric Review Analysis of Research on the Use of Waste Rubber Tyres in Building and Construction Materials", Polymers, 17(18), 2480, 2025. https://doi.org/10.3390/polym17182480

[25] Meddah, A., Beddar, M., Bali, A. "Use of Shredded Rubber-Tire Aggregates for Roller-Compacted Concrete Pavement", Journal of Cleaner Production, 72, pp. 187–192, 2014. https://doi.org/10.1016/j.jclepro.2014.02.052

[26] Fakhri, M., Amoosoltani, E. "The Effect of Reclaimed Asphalt Pavement and Crumb Rubber on Mechanical Properties of Roller-Compacted Concrete Pavement", Construction and Building Materials, 137, pp. 470–484, 2017. https://doi.org/10.1016/j.conbuildmat.2017.01.136

[27] Rezaifar, O., Hasanzadeh, M., Gholhaki, M. "Concrete Made with Hybrid Blends of Crumb Rubber and Metakaolin: Optimization Using Response Surface Method", Construction and Building Materials, 123, pp. 59–68, 2016. https://doi.org/10.1016/j.conbuildmat.2016.06.047

[28] Mohammed, B. S., Adamu, M., Liew, M. S. "Evaluating the Effect of Crumb Rubber and Nano-Silica on the Properties of High-Volume Fly-Ash Roller-Compacted Concrete Pavement Using Non-Destructive Techniques", Case Studies in Construction Materials, 8, pp. 380–391, 2018. https://doi.org/10.1016/j.cscm.2018.03.004

[29] Fakhri, M., Amoosoltani, E., Farhani, M., Ahmadi, A. "Determining Optimal Combination of RCCP Mixture Containing Recycled Asphalt Pavement and Crumb Rubber Using Hybrid ANN–GA Method Considering Energy-Absorbency Approach", Canadian Journal of Civil Engineering, 44(11), pp. 945–955, 2017. https://doi.org/10.1139/cjce-2017-0124

[30] Suryawanshi, N. T., Thakare, S. B. "Self-Curing Assessment of Meta Kaolin Based High Strength Concrete Using Super Absorbent Polymer", International Journal of Civil Engineering and Technology, 9(13), pp. 1082–1087, 2018.

[31] ASTM "ASTM C618-22 Standard Specification for Coal Fly Ash and Raw or Calcined Natural Pozzolan for Use in Concrete", ASTM International, West Conshohocken, PA, USA, 2022. https://doi.org/10.1520/C0618-22

[32] Uysal, M., Tanyildizi, H. "The Role of Fine Aggregates in RCC Mixtures", Journal of Materials in Civil Engineering, 24(5), pp. 556–563,2012. https://doi.org/10.1061/(ASCE)MT.1943-5533.0000427

[33] Tayabji, N., Okamoto, P. "Aggregate Influence on RCC Pavement Performance", Journal of Materials in Civil Engineering, 10(3), pp. 184–192, 1998.

[34] Piarc, X. "Gradation Optimization for RCC Dams", Concrete International, 15(6), pp. 42–48, 1993.

[35] ASTM "ASTM C494/C494M-24 Standard Specification for Chemical Admixtures for Concrete", ASTM International, West Conshohocken, PA, USA, 2024. https://doi.org/10.1520/C0494_C0494M-24

[36] ASTM "ASTM C1437-15 Standard Test Method for Flow of Hydraulic Cement Mortar", ASTM International, West Conshohocken, PA, USA, 2015. https://doi.org/10.1520/C1437-15

[37] ASTM "ASTM C31/C31M-12 Standard Practice for Making and Curing Concrete Test Specimens in the Field", ASTM International, West Conshohocken, PA, USA, 2012. https://doi.org/10.1520/C0031_C0031M-12

[38] ASTM "ASTM C511-13 Standard Specification for Mixing Rooms, Moist Cabinets, Moist Rooms, and Water Storage Tanks Used in the Testing of Hydraulic Cements and Concretes", ASTM International, West Conshohocken, PA, USA, 2013. https://doi.org/10.1520/C0511-13

[39] ASTM "ASTM C496/C496M-17 Standard Test Method for Splitting Tensile Strength of Cylindrical Concrete Specimens (Withdrawn 2026)", ASTM International, West Conshohocken, PA, USA, 2017.

[40] ASTM "ASTM C293/C293M-16 Standard Test Method for Flexural Strength of Concrete (Using Simple Beam With Center-Point Loading) (Withdrawn 2025)", ASTM International, West Conshohocken, PA, USA, 2016.

[41] ASTM "ASTM C642-06 Standard Test Method for Density, Absorption, and Voids in Hardened Concrete", ASTM International, West Conshohocken, PA, USA, 2006. https://doi.org/10.1520/C0642-06

[42] ACI Committee 318 "Building Code Requirements for Structural Concrete (ACI 318-11) and Commentary", American Concrete Institute, 2011.

[43] CEN "EN 1992-1-1:2004. Eurocode 2: Design of Concrete Structures – Part 1-1: General Rules and Rules for BuildingsEN 1992-1-1:2004", European Committee for Standardization, Brussels, Belgium, 2004.

[44] Standards New Zealand "NZS 3101: Part 1 – The Design of Concrete Structures (Amendment 3, 2017)", Standards New Zealand, Wellington, New Zealand, 2006.

[45] Japan Concrete Institute (JCI) "JCI Guidelines for Control of Cracking of Mass Concrete", Japan Concrete Institute, 2008.

[46] Standards Australia "AS 3600:2018 – Concrete Structures", Standards Australia, Sydney, Australia, 2018.